

# Signatures for strong-field QED physics in the quantum limit of beamstrahlung

W. L. Zhang,<sup>1,\*</sup> T. Grismayer,<sup>1,†</sup> and L. O. Silva<sup>1,‡</sup>

<sup>1</sup>*GoLP/Instituto de Plasmas e Fusão Nuclear, Instituto Superior Técnico, Universidade de Lisboa, Lisboa, Portugal*

(Dated: February 7, 2023)

Collisions between round ultrarelativistic leptonic beams are proposed to probe strong-field quantum electrodynamics (SF-QED) in the quantum limit of beamstrahlung. The collective radiation spectrum from a leptonic collision is derived. A characteristic spectral peak close to the beam energy is identified, as a signature predicted by SF-QED theory. The dependences of the spectral peak and beamstrahlung on the collision parameters are determined, paving the way to experimentally verify SF-QED. Ultrashort, ultrabright, and high-luminosity colliding gamma-ray beams are generated. The theoretical results are confirmed by self-consistent 3-dimensional QED particle-in-cell simulations.

Beamstrahlung (synchrotron radiation) in leptonic (electron or positron) collisions in future colliders can lead to severe energy loss of colliding beams [1–4]. Beamstrahlung can also be utilized to test the strong-field QED (SF-QED) theory. SF-QED describes the quantum dynamics of particles in strong fields [5–10], for which many open questions are still unsolved [11–15]. The quantum regime is characterized by  $\chi_e \gtrsim 1$ , where  $\chi_e = \sqrt{(\gamma\mathbf{E} + \mathbf{p}/mc \times \mathbf{B})^2 - (\mathbf{p}/mc \cdot \mathbf{E})^2}/E_s$  is the quantum (or beamstrahlung) parameter. Here,  $E_s = m^2c^3/e\hbar$  is the Sauter-Schwinger field,  $\hbar$  is the reduced Planck constant,  $c$  is the speed of light in vacuum,  $e$  and  $m$  are the charge and mass of an electron,  $\mathbf{p}$  and  $\gamma$  are the momentum and Lorentz factor of the particle, and  $\mathbf{E}$  and  $\mathbf{B}$  are the electric and magnetic fields. High-luminosity collisions between dense and high-energy (10's GeV to a few TeV) beams planned for future colliders, including advanced collider concepts through high-gradient plasma-based accelerators [1, 2, 16–21], will place beamstrahlung in the quantum or even deep quantum ( $\chi_e \gg 1$ ) regimes [12, 22–28].

The self fields of colliding beams are ideally suited for SF-QED: they are well-defined and quasi-static (non-oscillating in space and time), thus providing a highly controllable platform, as compared with laser-based configurations [29–46] and beam-plasma interactions [47]. The locally constant field approximation (LCFA) [5, 9, 10, 48–52], usually invoked in the SF-QED theory, is valid in leptonic collisions [12, 26]. In addition, beamstrahlung photons from beam-beam collisions are highly collimated, with divergence angles  $\lesssim 1$  mrad (as shown later), thus facilitating probing and diagnostics of SF-QED.

SF-QED theory describes the dynamics of single particles in first-order processes [9, 10], including nonlinear Compton scattering (responsible for beamstrahlung explored here) and nonlinear Breit-Wheeler electron-positron pair creation. The theory provides the local, instantaneous differential probability for a particle to undergo these processes. However, in (either laser- or beam-driven) experiments, the signatures, e.g., photons collected by the diagnostics, include the integrated contribution from all particles in the colliding beam(s). Del

Gaudio *et al.* [26] studied the beamstrahlung and pair creation from leptonic collisions in the weak quantum regime ( $\chi_e \lesssim 1$ ). Previous studies [22, 24], employing the mean field model and discarding the realistic field profiles, have shown deviations from the expected beamstrahlung spectrum in the  $\chi_e \lesssim 1$  regime [26]. The key properties of beamstrahlung in the  $\chi_e > 1$  regime, and the associated impact of spatial profiles of colliding beams, remain unexplored.

Recently, Tamburini *et al.* [27] proposed a specially designed, asymmetric collision configuration with the goal of studying the time-integrated single-particle radiation dynamics. This special configuration employs colliding beams with significantly different sizes and requires a special alignment, demanding advanced beam control and delivery, which are still far from experimental realization.

In this Letter, we generalize the beamstrahlung study to a broad quantum regime where  $\chi_e \gtrsim 1$ , by an analytical solution to the radiation spectrum from conventional collisions between symmetric, round beams. We show that these collisions can be utilized to explore the SF-QED theory. The transition of beamstrahlung from the mild quantum regime ( $\chi_e \sim 1$ ) to the SF-QED regime ( $\chi_e \gg 1$ ) with distinctive features is identified. This symmetric collision configuration was explored by Yakimenko *et al.* [12] to show that short and dense beam collisions can be used to enter the non-perturbative regime [11, 13–15, 39, 53], where  $\alpha\chi_e^{2/3} \gtrsim 1$  with  $\alpha$  being the fine-structure constant. Here, our study assumes  $\alpha\chi_e^{2/3} \ll 1$ , far from the challenges of the nonperturbative QED nature. We also assume that the pair creation is insignificant compared to the emitted photons, and beam disruption is negligible, i.e.,  $D \ll 1$ , where  $D = r_e N_0 \sigma_z / \gamma \sigma_0^2$  is the disruption parameter [54]. Here,  $r_e$  is the classical electron radius,  $N_0$ ,  $\sigma_z$ , and  $\sigma_0$  are the particle number, longitudinal length, and transverse size of the beam, respectively.

In our model, the colliding beams have Gaussian profiles, with the density characterized by  $n = n_0 f(r)g(z)$ . Here,  $n_0$  is the peak density,  $f(r) = \exp(-r^2/2\sigma_0^2)$ , where  $r$  is the radial position, assuming round (cylin-

drical) symmetry in the transverse direction.  $g(z) = \exp(-(z - z_c)^2/2\sigma_z^2)$ , where  $z$  is the longitudinal coordinate co-moving with the beam and  $z_c$  depicts the beam center. The radial electric and azimuthal magnetic fields of a round ultrarelativistic beam are given by  $E_r = 4\pi en_0 F(r)g(z)$  and  $B_\theta \simeq E_r$  [26], with  $F(r) = \int_0^r f(r')r'dr'/r$ . The local instantaneous  $\chi_e$  for a particle, under fields from the oncoming beam, is given by

$$\chi_e(r, t) \simeq \frac{2\gamma E_r}{E_s} = \frac{8\pi|e|n_0\gamma}{E_s} F(r) \exp(-u^2) \quad (1)$$

where  $u = \sqrt{2}ct/\sigma_z$  is the normalized time, and we have assumed that the particle under study crosses the center of the oncoming beam at  $t = 0$ . For a Gaussian beam,  $F(r) = \sigma_0^2(1 - \exp(-r^2/2\sigma_0^2))/r$ , and the fields peak at  $r = r_{peak} = 1.6\sigma_0$ , leading to the maximum  $\chi_e$  given by

$$\chi_{e\ max} = \chi_e(r_{peak}, 0) = 15.3 \frac{\mathcal{E}_0[10\ \text{GeV}]}{\sigma_0[0.1\ \mu\text{m}]} \frac{N_0[10^{10}]}{\sigma_z[0.1\ \mu\text{m}]} \quad (2)$$

where  $\mathcal{E}_0 = \gamma mc^2$  is the beam energy. Equation (2) shows that the  $\chi_e > 1$  regime can be reached by delivering high-energy ( $\mathcal{E}_0 > 10$  GeV) and submicron ( $\sigma_0 \lesssim \mu\text{m}$  and  $\sigma_z \lesssim \mu\text{m}$ ) beams with  $\sim$  nC charge.

The differential probability rate of photon emission in the quantum regime is given by [5]

$$\frac{d^2W}{dtd\xi} = \frac{\alpha}{\sqrt{3}\pi\tau_c\gamma} \left[ \text{Int}K_{5/3}(b) + \frac{\xi^2}{1-\xi} K_{2/3}(b) \right] \quad (3)$$

where  $\tau_c = \hbar/mc^2$  is the Compton time,  $\xi = \mathcal{E}_\gamma/\mathcal{E}_0$  with  $\mathcal{E}_\gamma$  the photon energy,  $b = 2/(3\chi_e(r, t))\xi/(1-\xi)$  and  $\text{Int}K_{5/3}(b) = \int_b^\infty K_{5/3}(q)dq$ , with  $K_\nu$  the modified Bessel function of the second kind. The condition for the validity of LCFA in a leptonic collision is analyzed in the Supplemental Material [55]. The LCFA has also been verified to be valid for the conditions considered in our study. The time-integrated photon spectrum emitted from a single particle in a beam is given by  $s_\omega(\xi, r) = \int_{-\infty}^\infty (d^2W/dtd\xi)dt$  [26]. The collective spectrum from the whole beam, normalized by the particle number  $N_0$ , is given by  $\mathcal{S}_\omega(\xi) = \int_0^\infty s_\omega(\xi, r)f(r)rdr / \int_0^\infty f(r)rdr$ .

In order to obtain analytical results for  $\mathcal{S}_\omega(\xi)$ , we will consider two assumptions. We approximate the special functions in  $d^2W/dtd\xi$  [Eq. (3)], such that  $K_{2/3}(b) \simeq k_{2/3}b^{-2/3}\exp(-b)$  and  $\text{Int}K_{5/3} \simeq 2K_{2/3}(b) \simeq 2k_{2/3}b^{-2/3}\exp(-b)$ , where  $k_{2/3} = 1.23$  is a fitting coefficient. To perform the double integral in  $\mathcal{S}_\omega(\xi)$ , we also approximate the density profile as a uniform profile. Since it is important to preserve the  $\chi_e$  distribution of particles in the collision ( $dN/d\chi_e$ ), we approximate the Gaussian profiles by a uniform cylinder of radius  $\sigma_{0A}$  and length  $\sigma_{zA} = 2\sqrt{2}\sigma_z$ , with a constant density  $n_{0A}$ . It is crucial to preserve the  $dN/d\chi_e$  distribution of beam particles, as the radiation probability [Eq. (3)] is solely

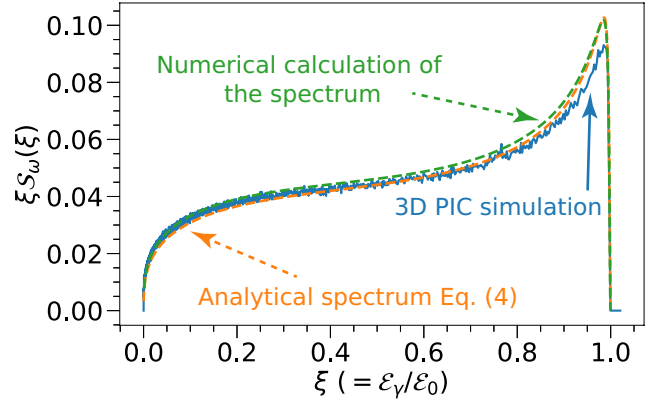


FIG. 1. (Color online). The normalized collective energy spectrum  $\xi\mathcal{S}_\omega(\xi)$  of photon radiation from a head-on collision between two identical, cold, round, and Gaussian electron beams with  $\chi_{e\ max} = 200$ . Each beam has energy  $\mathcal{E}_0 = 90$  GeV, longitudinal length  $\sigma_z = 30.7$  nm, transverse size  $\sigma_0 = 30.7$  nm, and particle number  $N_0 = 1.37 \times 10^9$ . The blue line is for a 3D PIC simulation. The orange dashed line is for the analytical spectrum Eq. (4). The green dashed line is for the numerical calculation of  $\mathcal{S}_\omega(\xi)$  without employing approximations, i.e., using exact  $d^2W/dtd\xi$  in Eq. (3) and the original Gaussian beam profile.

determined by  $\chi_e(r, t)$  of the emitting particle. We further impose the requirement that the approximated uniform profile should match  $\chi_{e\ max}$  of the original Gaussian profiles, leading to  $n_{0A}\sigma_{0A} = 0.9n_0\sigma_0$ . These approximations are detailed and justified in the Supplemental Material [55]. With these approximations,  $\mathcal{S}_\omega(\xi)$  is given by

$$\mathcal{S}_\omega(\xi) = \frac{2\sqrt{2}\alpha\sigma_z}{\sqrt{3}\pi\tau_c\gamma c} k_{2/3} \left( 2 + \frac{\xi^2}{1-\xi} \right) b_0^2 \Gamma \left[ -\frac{8}{3}, b_0 \right] \quad (4)$$

where  $b_0 = 2/(3\chi_{e\ max})\xi/(1-\xi)$  and  $\Gamma$  is the incomplete Gamma function [56, 57]. The detailed derivation is provided in the Supplemental Material [55]. Equation (4) is verified to give the accurate photon emission in both the  $\chi_{e\ max} \sim 1$  and the  $\chi_{e\ max} > 1$  regimes. On the other hand, we found that the beamstrahlung spectrum [24] obtained using the mean field model severely underestimates the photon emission in the  $\chi_{e\ max} > 1$  regime, indicating that the realistic beam and field profiles should be taken into account for the beamstrahlung study in the quantum regime.

The typical energy spectrum  $\xi\mathcal{S}_\omega(\xi)$  from a head-on collision between symmetric, round, and Gaussian leptonic beams is shown in Fig. 1 for an electron-electron collision with  $\chi_{e\ max} = 200$ . The disruption effect in this collision is negligible, as  $D = 7 \times 10^{-4} \ll 1$ . The analytical spectrum Eq. (4) is in excellent agreement with the direct numerical calculation of  $\mathcal{S}_\omega(\xi)$  using the Gaussian profiles. 3-dimensional (3D) particle-in-cell (PIC) simulations with OSIRIS [58], where SF-QED effects are

self-consistently included [33, 59, 60], also confirm our analytical results. The simulation details are provided in the Supplemental Material [55]. The simulation for this particular scenario shows that only 3% of photon energy is transferred to pairs, indicating that pair creation is insignificant, as assumed in our theoretical model. The beam-to-photon conversion efficiency (i.e., beam loss)  $\eta_\gamma$  is given by  $\eta_\gamma = \int_0^1 \xi \mathcal{S}_\omega(\xi) d\xi$ . For the collision in Fig. 1, the analytical spectrum Eq. (4) gives  $\eta_\gamma = 4.8\%$ , in excellent agreement with the simulation. The analytical solution to  $\eta_\gamma$  will be given later (using Eq. (7)).

Using the analytical spectrum Eq. (4), we can identify the transition of beamstrahlung dynamics from the mild quantum regime ( $\chi_e \sim 1$ ) to the deep SF-QED regime ( $\chi_e \gg 1$ ); this transition is defined by a threshold quantum parameter  $\chi_{\text{thr}} = 40$ . When  $1 \lesssim \chi_{e \text{ max}} < \chi_{\text{thr}}$ , the yield of high-energy ( $\xi \sim 1$ ) photons grows with  $\chi_{e \text{ max}}$ , forming a plateau-like high-energy tail in the photon spectrum ( $\mathcal{S}_\omega(\xi)$ ). The energy spectrum ( $\xi \mathcal{S}_\omega(\xi)$ ) is also broadband. When  $\chi_{e \text{ max}} > \chi_{\text{thr}}$ , a distinctive, sharp peak close to the beam energy appears in the  $\mathcal{S}_\omega(\xi)$  spectrum, as well as in the  $\xi \mathcal{S}_\omega(\xi)$  spectrum as shown in Fig. 1, where the peak is at  $\xi_{\text{peak}} = 0.985$ . This peak shows that the collective beamstrahlung spectrum from a collision preserves the characteristic spectral peak of single particles, resulting from  $d^2W/dtd\xi$  [Eq. (3)] for particles with  $\chi_e > 16$ , and first identified in [8, 27, 61]. The distinctive spectral peak identified here opens the way to experimental exploration of SF-QED dynamics using beam collisions. The increased threshold  $\chi_{\text{thr}}$  is due to the realistic temporal and spatial beam profiles. Physically, a fraction of the beam particles samples a  $\chi_e(r, t)$  [Eq. (1)] which is below the threshold  $\chi_e (= 16)$  predicted for the peak in the single-particle spectrum, leading to the higher threshold  $\chi_{\text{thr}} = 40$  for realistic beam collisions.

The characteristic spectral peak can be determined from Eq. (4) by solving  $\partial_{b_0}(\xi \mathcal{S}_\omega(\xi)) = 0$ . The peak position  $b_{0, \text{peak}} = 2/(3\chi_{e \text{ max}})\xi_{\text{peak}}/(1 - \xi_{\text{peak}})$  converges to an asymptotic value, i.e.,  $b_{0, \text{peak}} \rightarrow 0.229$ , when  $\chi_{e \text{ max}}$  increases. Assuming  $b_{0, \text{peak}} \simeq 0.229$ , Eq. (4) determines the amplitude of the spectral peak,  $P_{\xi \mathcal{S}_\omega}$ , which scales as

$$P_{\xi \mathcal{S}_\omega} = 0.155 \frac{\alpha \sigma_z}{\tau_c \gamma c} \chi_{e \text{ max}} = 0.15 \frac{\sigma_z [0.1 \mu\text{m}]}{\mathcal{E}_0 [\text{GeV}]} \chi_{e \text{ max}} \quad (5)$$

Since  $\xi_{\text{peak}} \simeq 1$ ,  $P_{\xi \mathcal{S}_\omega}$  [Eq. (5)] can also be used to evaluate the peak amplitude in the  $\mathcal{S}_\omega$  spectrum,  $P_{\mathcal{S}_\omega}$ , i.e.,  $P_{\mathcal{S}_\omega} \simeq P_{\xi \mathcal{S}_\omega}$ . We have confirmed Eq. (5) by comparing with the peak in the numerical  $\xi \mathcal{S}_\omega$  spectrum (e.g., green line in Fig. 1), as illustrated in Fig. 2 where  $P_{\xi \mathcal{S}_\omega}$  is verified to linearly depend on  $\chi_{e \text{ max}}$  when  $\sigma_z$  and  $\gamma$  are fixed.

Conventional collisions between symmetric round beams can be used to probe the SF-QED physics by examining the characteristic peak in the beamstrahlung spectrum. Our study shows that the characteristic spectral peak can subsist in a collision where beam particles

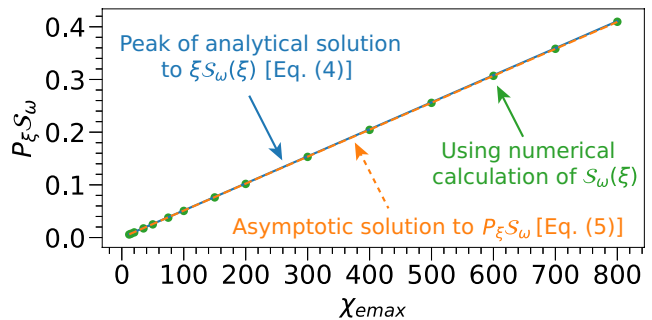


FIG. 2. (Color online). Scaling of the peak amplitude  $P_{\xi \mathcal{S}_\omega}$  of the energy spectrum ( $\xi \mathcal{S}_\omega(\xi)$ ) with  $\chi_{e \text{ max}}$  in the  $\chi_{e \text{ max}} \gg 1$  regime. Here,  $\chi_{e \text{ max}}$  is varied by adjusting the corresponding  $\sigma_0$  of the colliding beams. Other beam parameters ( $n_0$ ,  $\mathcal{E}_0$ , and  $\sigma_z$ ) are the same with the collision in Fig. 1. The green circles show the peak of  $\xi \mathcal{S}_\omega(\xi)$  spectrum obtained using numerical calculation. The blue line shows the peak of analytical  $\xi \mathcal{S}_\omega(\xi)$  spectrum [Eq. (4)]. The orange dashed line shows the asymptotic solution to  $P_{\xi \mathcal{S}_\omega}$  [Eq. (5)].

emit less than one photon on average. This requirement can be formulated as  $\overline{N}_\gamma < 1$ , where  $\overline{N}_\gamma = N_\gamma/N_0 = \int_0^1 \mathcal{S}_\omega(\xi) d\xi$  is the averaged number of photon emission from a beam particle, with  $N_\gamma$  the number of photons. If  $\overline{N}_\gamma > 1$ , multiphoton emission and significant pair creation occur, suppressing the spectral peak. This is consistent with the single-particle dynamics where the spectral peak appears when one-photon emission dominates [27]. Using Eq. (4), in the limit of  $\chi_{e \text{ max}} \gg 1$ ,  $\overline{N}_\gamma$  is given by  $\overline{N}_\gamma \simeq 1.88 \alpha \sigma_z \chi_{e \text{ max}}^{2/3} / \tau_c \gamma c$ . The condition  $\overline{N}_\gamma < 1$  then determines the required collision parameters as

$$\overline{N}_\gamma \simeq 1.82 \frac{\sigma_z [0.1 \mu\text{m}]}{\mathcal{E}_0 [\text{GeV}]} \chi_{e \text{ max}}^{2/3} < 1 \quad (6)$$

The averaged rate of photon emission from a beam particle in the collision process is  $d\overline{N}_\gamma/dt \simeq \overline{N}_\gamma / (\sqrt{2}\sigma_z/c) = 1.33\alpha / (\tau_c \gamma) \chi_{e \text{ max}}^{2/3}$ . The scaling of  $d\overline{N}_\gamma/dt$  is identical to the instantaneous rate of photon emission from a particle in the  $\chi_e \gg 1$  limit [9]. This shows that the beamstrahlung dynamics of a collision is characterized by the corresponding  $\chi_{e \text{ max}}$ , and shares the same scaling as with single-particle dynamics. Similarly, using Eq. (4), the averaged energy  $\overline{\mathcal{E}}_\gamma$  radiated from a beam particle,  $\overline{\mathcal{E}}_\gamma = \int_0^1 \mathcal{E}_0 \xi \mathcal{S}_\omega(\xi) d\xi$ , can be obtained as

$$\overline{\mathcal{E}}_\gamma \simeq 0.47 \frac{\alpha m c^2 \sigma_z}{\tau_c c} \chi_{e \text{ max}}^{2/3} \simeq \frac{\overline{N}_\gamma}{4} \mathcal{E}_0 \quad (7)$$

With Eq. (7), the beam-to-photon conversion efficiency is given by  $\eta_\gamma = \overline{\mathcal{E}}_\gamma / \mathcal{E}_0 \simeq \overline{N}_\gamma / 4$ , indicating a low beam loss when  $\overline{N}_\gamma < 1$ . The averaged radiation power from a beam particle in the collision process is then  $\overline{P}_{\text{rad}} \simeq \overline{\mathcal{E}}_\gamma / (\sqrt{2}\sigma_z/c) = 0.33(\alpha m c^2 / \tau_c) \chi_{e \text{ max}}^{2/3}$ . We note that the total radiated energy is  $\mathcal{E}_\gamma^{\text{tot}} = N_0 \overline{\mathcal{E}}_\gamma \propto$

$(\mathcal{E}_0\sqrt{\sigma_z}/\sigma_0)^{2/3}N_0^{5/3}$ , showing a strong dependence with the particle number as  $\propto N_0^{5/3}$ .

Our estimations for  $\overline{N}_\gamma$  and  $\overline{\mathcal{E}}_\gamma$  are confirmed by 3D PIC simulations. The averaged number of pair creation from a beam particle in a collision  $\overline{N}_p = N_p/N_0$ , where  $N_p$  is the number of pair creation, can also be estimated as follows. The rate of pair creation can be approximated by  $d\overline{N}_p/dt \simeq 0.38\alpha\chi_{e\max}^{2/3}/\tau_c\gamma$  in the  $\chi_e \gg 1$  regime [9, 62].  $N_p$  is then  $N_p \sim N_\gamma(d\overline{N}_p/dt)(\sqrt{2}\sigma_z/c) \simeq 0.28\overline{N}_\gamma^2 N_0$ . Since  $\overline{N}_p \propto \overline{N}_\gamma^2$ , pair creation is negligible when  $\overline{N}_\gamma < 1$ , and our analysis for beamstrahlung holds. However, if  $\overline{N}_\gamma \gtrsim 1$ , pair creation will become significant and needs to be taken into account for beamstrahlung in the  $\chi_{e\max} > 1$  regime.

Our study also applies to collisions between beams with finite emittance and energy spread. Because the collision duration is short, the transverse emittance has negligible impact on the particle trajectory and photon emission. PIC simulations show that the photon spectrum in Fig. 1 remains unchanged when the beams are set to have a significant normalized emittance up to  $\varepsilon_N \sim 27$  mm mrad (this is comparable to  $\varepsilon_N$  for the self-injected beams from laser wakefield acceleration [63]). On the other hand, the energy spread  $\Delta\mathcal{E}_0$  of the colliding beams is found to mainly affect (broaden) the characteristic spectral peak, because  $\Delta\mathcal{E}_0$  results in a spread in  $\chi_{e\max}$  according to Eq. (2). 3D PIC simulations show that the well-defined spectral peak can be observed for relative energy spreads  $\Delta\mathcal{E}_0/\mathcal{E}_0 < 5\%$ .

Our study indicates that for the expected signature of spectral peak to be observed, the leptonic collisions are required to satisfy

$$\frac{\sigma_z[0.1\mu m]}{\mathcal{E}_0[\text{GeV}]} < 0.038 \frac{N_0[10^{10}]}{\sigma_0[0.1\mu m]} \quad (\text{for } \chi_{e\max} > \chi_{\text{thr}}) \quad (8a)$$

$$\frac{\sigma_z[0.1\mu m]}{\mathcal{E}_0[\text{GeV}]} < 0.07 \left( \frac{\sigma_0[0.1\mu m]}{N_0[10^{10}]} \right)^2, \quad \Delta\mathcal{E}_0/\mathcal{E}_0 < 5\%, \quad (8b)$$

where  $\chi_{\text{thr}} = 40$  (analyzed before), and Eq. (8b) comes from the condition  $\overline{N}_\gamma < 1$  [Eq. (6)] and the requirement of energy spread, respectively. For example, if one employs leptonic beams with  $\mathcal{E}_0 = 30$  GeV and  $\sim$  nC charge, Eq. (8) indicates that submicron beam sizes are preferred. If  $\sigma_0$  is assumed to be  $\sigma_0 = 0.05 \mu m$ , one has  $\sigma_z < 0.13 \mu m$ .

The disruption effect in leptonic collisions can be related to beamstrahlung via  $\overline{N}_\gamma \simeq 1.51\alpha^{4/3}N_0^{1/3}D^{1/3}$ . With conventional  $\sim$  nC beams ( $N_0 \gtrsim 10^9$ ), if  $\overline{N}_\gamma < 1$  (as required by our study) is satisfied, one will have  $D \ll 1$ , indicating that disruption can be safely neglected in our study. One can enter the mild-disruption regime where  $\overline{N}_\gamma < 1$  and  $D \sim 1$ , using transversely compressed ( $\sigma_0 \lesssim$  nm),  $\sim$  pC ( $N_0 \sim 10^7$ ) beams. We briefly investigated this regime with 3D PIC simulations, for typical parameters of an electron-electron collision

where  $\overline{N}_\gamma \simeq 0.5$ ,  $D = 1$ , and  $\chi_{e\max} = 100$ , using beams with  $\mathcal{E}_0 = 90$  GeV,  $N_0 = 1.28 \times 10^7$ ,  $\sigma_0 = 0.15$  nm,  $\sigma_z = 115$  nm. The colliding beams expel each other, leading to the drop of beam densities and fields. However, this mild disruption does not fundamentally change our theoretical predictions. The simulations suggest that the emitted photon spectrum approximately agrees with our model [Eq. (4)], with a reduced characteristic spectral peak. The disruption also leads to a drop in the photon energy by  $\lesssim 20\%$  compared to our theory [Eq. (7)].

The coupled regime between the disruption and beamstrahlung will be entered when  $\overline{N}_\gamma > 1$ . In this regime, multiphoton emission occurs, leading to considerable beam loss  $\eta_\gamma$  [Eq. (7)]. Since the beam energy significantly decreases during the collision,  $D (\propto \gamma^{-1})$  will dynamically increase. Therefore, the disruption will come into play, even when the initial disruption ( $D_0$ ) is negligible ( $D_0 \ll 1$ ). As  $\overline{N}_p \propto \overline{N}_\gamma^2$  (analyzed before), the pair creation also becomes significant. The created pair particles, carrying lower energy, are more susceptible to the background fields, and will thus experience strong transverse pinch or repulsion. In the regime where  $\overline{N}_\gamma > 1$  and  $D_0 \gtrsim 1$ , the disruption and beamstrahlung are strongly coupled [28], and this regime will be explored in future works.

Ultrashort ( $\lesssim$  fs), ultrabright colliding gamma-ray beams are produced in the collision. The gamma-ray beam is highly collimated along the propagation direction of the emitting beam. The divergence angle of the gamma-ray beam is  $\theta_0 \sim D\sigma_0/\sigma_z \ll 1$  [54]. For the collision with  $\chi_{e\max} = 200$  shown in Fig. 1,  $\theta_0 \lesssim 1$  mrad. The spectral brightness  $B(\xi)$  is found to be  $\propto \xi\mathcal{S}_\omega(\xi)$ . Therefore,  $B(\xi)$  also features a sharp peak  $B_{\text{peak}}$  at  $\xi = \xi_{\text{peak}}$ . The PIC simulation shows  $B_{\text{peak}} \simeq 6.16 \times 10^{30}$  photons/(s mm<sup>2</sup> mrad<sup>2</sup> 0.1%BW). These ultrabright gamma-ray beams, at 100 GeV-level photon energies ( $\mathcal{E}_\gamma \simeq \mathcal{E}_0$ ), are expected to have multiple unprecedented applications [64–67]. The peak spectral brightness  $B_{\text{peak}}$  can be estimated as

$$\frac{B_{\text{peak}}(\xi_{\text{peak}})}{\text{photons}/(\text{s mm}^2 \text{ mrad}^2 \text{ 0.1\%BW})} \simeq 1.16 \times 10^{26} \frac{(\mathcal{E}_0[\text{GeV}])^2}{\sigma_0[0.1\mu m] \sigma_z[0.1\mu m]}. \quad (9)$$

Equation (9) provides a good estimation for the peak brightness of beamstrahlung photons in both  $\chi_{e\max} \sim 1$  and  $\chi_{e\max} > 1$  regimes. The detailed analysis and derivations of  $B_{\text{peak}}$  are given in the Supplemental Material [55].

The luminosity of the emitted colliding gamma-ray beams  $L_{\gamma\gamma}$  is high, and can be estimated based on the photon yield, i.e.,  $L_{\gamma\gamma}^{\text{estimate}} \sim \overline{N}_\gamma^2 L_{e-e-}$  where  $L_{e-e-}$  is the electron luminosity, given by  $N_0^2/4\pi\sigma_0^2$  when the disruption is negligible [54, 68]. For the condition in Fig. 1,

the simulations give  $L_{\gamma\gamma} \simeq 0.01L_{e^-e^-}$  (for photons with  $\mathcal{E}_\gamma > 1$  MeV), also in agreement with our estimation.

In summary, the beamstrahlung dynamics in leptonic collisions is studied for the  $\chi_e \gtrsim 1$  regime, both with a model and self-consistent 3D PIC simulations. The analytical spectrum is determined for beamstrahlung from collisions between symmetric round beams. It demonstrates that these collisions preserve the characteristic spectral peak predicted for single-particle radiation dynamics, at a higher  $\chi_{\text{thr}}$ . The features of the photon radiation and their dependences are fully determined. Our study shows that collisions between round beams can be utilized to explore the SF-QED theory, by probing the resulting beamstrahlung spectrum. We also show that ultrashort ( $\lesssim$  fs), ultrabright, highly collimated, and high-luminosity colliding gamma-ray beams, at 100 GeV-level photon energies, can be produced through these collisions. This work also opens two new directions. Firstly, the spectral gamma-ray luminosity, i.e.,  $L_{\gamma\gamma}(\mathcal{E}_\gamma)$ , can be further examined, using our results [24]. Secondly, the beamstrahlung analysis in this Letter can be generalized to include the spin and polarization of beam particles and photons [69–77].

This work was supported by the European Research Council (ERC-2015-AdG grant No. 695088), and FCT (Portugal) Grants No. UIDB/FIS/50010/2020 - PESTB 2020-23. We acknowledge PRACE for awarding us access to MareNostrum at Barcelona Supercomputing Center (BSC, Spain). Simulations were performed at the IST cluster (Lisbon, Portugal) and at MareNostrum.

---

\* wenlong.zhang@tecnico.ulisboa.pt

† thomas.grismayer@tecnico.ulisboa.pt

‡ luis.silva@tecnico.ulisboa.pt

- [1] V. D. Shiltsev, *Phys.-Usp.* 55, 965 (2012).
- [2] V. Shiltsev and F. Zimmermann, *Rev. Mod. Phys.* 93, 015006 (2021).
- [3] H. M. Gray, *Reviews in Physics* 6, 100053 (2021).
- [4] European Strategy Group, 2020 Update of the European Strategy for Particle Physics (Brochure), Tech. Rep. CERN-ESU-015, Geneva, 2020, <https://cds.cern.ch/record/2721370>
- [5] V. I. Ritus, Quantum effects of the interaction of elementary particles with an intense electromagnetic field, *J. Sov. Laser Res.* 6, 497 (1985).
- [6] V. N. Baier, V. M. Katkov, and V. M. Strakhovenko, *Electromagnetic Processes at High Energies in Oriented Single Crystals* (World Scientific, Singapore, 1998).
- [7] A. Di Piazza, C. Müller, K. Z. Hatsagortsyan, and C. H. Keitel, *Rev. Mod. Phys.* 84, 1177 (2012).
- [8] S. S. Bulanov, C. B. Schroeder, E. Esarey, and W. P. Leemans, *Phys. Rev. A* 87, 062110 (2013).
- [9] A. Gonoskov, et al., *Rev. Mod. Phys.* 94, 045001 (2022).
- [10] A. Fedotov, et al., arXiv:2203.00019 (2022).
- [11] A. M. Fedotov, *J. Phys. Conf. Ser.* 826, 012027 (2017).
- [12] V. Yakimenko, et al., *Phys. Rev. Lett.* 122, 190404 (2019).
- [13] A. Ilderton, *Phys. Rev. D* 99, 085002 (2019).
- [14] A. A. Mironov, S. Meuren, and A. M. Fedotov, *Phys. Rev. D* 102, 053005 (2020).
- [15] T. Heinzl, A. Ilderton, and B. King, *Phys. Rev. Lett.* 127, 061601 (2021).
- [16] FACET-II Technical Design Report No. SLAC-R-1072 (2016).
- [17] E. Adli, A. Ahuja, O. Apsimon, et al., *Nature* 561, 363 (2018).
- [18] ALEGRO collaboration, Towards an Advanced Linear International Collider, arXiv:1901.10370 (2019).
- [19] European Strategy for Particle Physics, Accelerator R&D Roadmap, CERN-2022-001, 2022.
- [20] T. Roser, et al., Report of the Snowmass’21 Collider Implementation Task Force, FERMILAB-FN-1184-AD-PPD, arXiv:2208.06030v1 (2022).
- [21] C. Clarke, et al., *JINST* 17, T05009 (2022).
- [22] R. J. Noble, *Nuclear Instruments and Methods in Physics Research Section A*, 256, 427 (1987).
- [23] P. Chen and V. I. Telnov, *Phys. Rev. Lett.* 63, 1796 (1989).
- [24] P. Chen, *Phys. Rev. D* 46, 1186 (1992).
- [25] K. Yokoya, P. Chen, "Beam-beam phenomena in linear colliders." *Frontiers of Particle Beams: Intensity Limitations. Lecture Notes in Physics*, vol. 400, pp. 415, 1992, Springer, Berlin, Heidelberg.
- [26] F. Del Gaudio, et al., *Physical Review Accelerators and Beams*, 22, 023402 (2019).
- [27] M. Tamburini and S. Meuren, *Phys. Rev. D* 104, L091903 (2021).
- [28] A. S. Samsonov, et al., *New J. Phys.* 23, 103040 (2021).
- [29] C. Bula, et al., *Phys. Rev. Lett.* 76, 3116 (1996).
- [30] D. L. Burke, et al., *Phys. Rev. Lett.* 79, 1626 (1997).
- [31] T. G. Blackburn, et al., *Phys. Rev. Lett.* 112, 015001 (2014).
- [32] A. Di Piazza, *Phys. Rev. Lett.* 117, 213201 (2016).
- [33] M. Vranic, et al., *New J. Phys.* 18, 073035 (2016).
- [34] M. Lobet, et al., *Phys. Rev. Accel. Beams* 20, 043401 (2017).
- [35] S. Gales, et al., *Rep. Prog. Phys.* 81, 094301 (2018).
- [36] K. Poder, et al., *Phys. Rev. X* 8, 031004 (2018).
- [37] F. Niel, et al., *Plasma Phys. Control. Fusion* 60, 094002 (2018).
- [38] J. M. Cole, et al., *Phys. Rev X* 8, 011020 (2018).
- [39] C. Baumann, et al., *Sci. Rep.* 9, 9407 (2019).
- [40] F. Albert, et al., *New J. Phys.* 23, 031101 (2021).
- [41] G. Hu, et al., *Phys. Rev. A* 102, 042218 (2020).
- [42] L. Fedeli, et al., *Phys. Rev. Lett.* 127, 114801 (2021).
- [43] Kenan Qu, Sebastian Meuren, and Nathaniel J. Fisch, *Phys. Rev. Lett.* 127, 095001 (2021).
- [44] M. Grech, et al., Investigating strong-field QED processes in laser-electron beam collisions at Apollon. hal-03229914, 2021.
- [45] A. Golub, S. Villalba-Chávez, and C. Müller, *Phys. Rev. D* 105, 116016 (2022).
- [46] M. Turner, et al., *Eur. Phys. J. D* 76, 205 (2022).
- [47] A. Matheron, et al., arXiv:2209.14280 (2022).
- [48] A. Di Piazza, et al., *Phys. Rev. A* 98, 012134 (2018).
- [49] A. Di Piazza, M. Tamburini, S. Meuren, and C. H. Keitel, *Phys. Rev. A* 99, 022125 (2019).
- [50] A. Ilderton, B. King, and D. Seipt, *Phys. Rev. A* 99, 042121 (2019).
- [51] B. King, *Phys. Rev. A* 101, 042508 (2020).

- [52] Q. Z. Lv, et al., Phys. Rev. Research 3, 013214 (2021).
- [53] V. I. Ritus, Radiative corrections in quantum electrodynamics with intense field and their analytical properties, Ann. Phys. (N.Y.) 69, 555 (1972).
- [54] P. Chen and K. Yokoya, Phys. Rev. D, 38, 987 (1988).
- [55] Supplemental Material for the details of the analytical solution to the collective beamstrahlung spectrum  $\mathcal{S}_\omega(\xi)$  from leptonic collisions in the quantum regime, 3-dimensional (3D) particle-in-cell (PIC) simulations for leptonic collisions, analysis of the validity of LCFA in leptonic collisions, and theoretical estimation of the spectral brightness of the gamma-ray photon beams emitted from leptonic collisions.
- [56] Incomplete Gamma and Related Functions, Chapter 8, NIST Handbook of Mathematical Functions, Edited by Frank W. J. Olver, Daniel W. Lozier, Ronald F. Boisvert and Charles W. Clark. Cambridge University Press, 2010.
- [57] R. B. Paris, Incomplete Gamma and Related Functions, NIST Digital Library of Mathematical Functions, <https://dlmf.nist.gov/8>
- [58] R. A. Fonseca, L. O. Silva, F. S. Tsung, V. K. Decyk, W. Lu, C. Ren, W. B. Mori, S. Deng, S. Lee, T. Katsouleas, and J. C. Adam, in Computational Science ICCS 2002, Lecture Notes in Computer Science (Springer, Berlin, Heidelberg, 2002), pp. 342–351.
- [59] T. Grismayer, et al., Phys. Plasmas 23, 056706 (2016).
- [60] T. Grismayer, et al., New J. Phys. 23, 095005 (2021).
- [61] J. Esberg and U. I. Uggerhøj, J. Phys. 198, 012007 (2009).
- [62] K. M. Schoeffler, et al., ApJ 870, 49 (2019).
- [63] S. F. Martins, R. A. Fonseca, W. Lu, et al., Nature Phys. 6, 311 (2010).
- [64] D. Asner, et al., Eur. Phys. J. C. 28, 27 (2003).
- [65] V. I. Telnov, JINST, 13 P03020 (2018).
- [66] T. Takahashi, Rev. Accel. Sci. Technol. 10, 215 (2019).
- [67] T. Barklow, et al., arXiv:2203.08484 (2022).
- [68] H. Wiedemann, Particle accelerator physics (3rd ed.), Springer Berlin, Heidelberg, 2007.
- [69] K. Yokoya and P. Chen, AIP Conference Proceedings 187, 938 (1989).
- [70] D. Del Sorbo, et al., Plasma Phys. Control. Fusion, 60, 064003 (2018).
- [71] Y.-F. Li, et al., Phys. Rev. Lett. 122, 154801 (2019).
- [72] H.-H. Song, W.-M. Wang, and Y.-T. Li, Phys. Rev. Research 3, 033245 (2021).
- [73] Yuhui Tang, et al., Phys. Rev. A 103, 042807 (2021).
- [74] Z. Gong, K. Z. Hatsagortsyan, and C. H. Keitel, Phys. Rev. Lett. 127, 165002 (2021).
- [75] D. Seipt, et al., New J. Phys. 23, 053025 (2021).
- [76] H. Baer, et al., The International Linear Collider Technical Design Report - Volume 2: Physics, arXiv:1306.6352 (2013).
- [77] I. Chaikovska, et al., JINST 17, P05015 (2022).
- [78] W. L. Zhang, et al., Phys. Rev. E 103, 013206 (2021).

---

## Supplemental Material: Signatures for strong-field QED physics in the quantum limit of beamstrahlung

W. L. Zhang, T. Grismayer, and L. O. Silva

*GoLP/Instituto de Plasmas e Fusão Nuclear, Instituto Superior Técnico, Universidade de Lisboa, Lisboa, Portugal*

Email: wenlong.zhang@tecnico.ulisboa.pt

### I. ANALYTICAL SOLUTION TO THE COLLECTIVE SPECTRUM $\mathcal{S}_\omega(\xi)$ OF PHOTON RADIATION FROM A COLLISION BETWEEN SYMMETRIC AND ROUND LEPTONIC BEAMS IN THE QUANTUM REGIME ( $\chi_e \gtrsim 1$ )

In this Section, we derive the analytical solution to the collective spectrum  $\mathcal{S}_\omega(\xi)$  of photon radiation from a collision between symmetric and round leptonic beams in the quantum regime, i.e.,  $\chi_e \gtrsim 1$ , where  $\chi_e$  is the quantum parameter (also called beamstrahlung parameter) defined in the main text.

In our model, the colliding beams have Gaussian profiles, with the density characterized by  $n = n_0 f(r)g(z)$ . Here,  $n_0$  is the peak density,  $f(r) = \exp(-r^2/2\sigma_0^2)$  is the transverse profile, assuming round (cylindrical) symmetry, where  $r$  is the radial position and  $\sigma_0$  is the transverse size of the beam.  $g(z) = \exp(-(z - z_c)^2/2\sigma_z^2)$  is the longitudinal profile, where  $z$  is the longitudinal coordinate co-moving with the beam (see Ref. [54] for details of the associated coordinate system used for collision study),  $\sigma_z$  is the longitudinal length of the beam,  $z_c$  depicts the beam center. The radial electric and azimuthal magnetic fields of a round ultrarelativistic beam are given by  $E_r = 4\pi en_0 F(r)g(z)$  and  $B_\theta = \beta E_r \simeq E_r$  [26], with  $F(r) = \int_0^r f(r')r' dr'/r$ . Here,  $e$  is the charge of an electron.  $\beta = v/c$  is the normalized beam velocity, where  $c$  is the speed of light in vacuum. The local instantaneous  $\chi_e$  for a particle, under fields from the oncoming beam, is given by

$$\chi_e(r, t) \simeq \frac{2\gamma E_r}{E_s} = \frac{8\pi|e|n_0\gamma}{E_s} F(r) \exp(-u^2) \quad (\text{S1})$$

where  $u = \sqrt{2}ct/\sigma_z$  is the normalized time, and we have assumed that the particle under study crosses the center of the oncoming beam at  $t = 0$ .  $E_s = m^2 c^3 / e\hbar$  is the Sauter-Schwinger field, where  $\hbar$  is the reduced Planck constant and  $m$  is the mass of an electron.  $\gamma = 1/\sqrt{1 - \beta^2} = \mathcal{E}_0/mc^2$  where  $\mathcal{E}_0$  is the beam energy. We assume that the fields peak

at  $r = r_{peak}$ , and the maximum  $\chi_e$  in the collision is given by  $\chi_{e\ max} = \chi_e(r_{peak}, 0)$ . For a Gaussian beam,  $\chi_{e\ max}$  is given in the main text.

The differential probability rate of photon emission in the quantum regime is given by [5]

$$\frac{d^2W}{dtd\xi} = \frac{\alpha}{\sqrt{3}\pi\tau_c\gamma} \left[ \text{Int}K_{5/3} + \frac{\xi^2}{1-\xi}K_{2/3}(b) \right] \quad (\text{S2})$$

Here,  $\xi = \mathcal{E}_\gamma/\mathcal{E}_0$  where  $\mathcal{E}_\gamma$  is the energy of the radiated photon.  $\tau_c = \hbar/mc^2$  is the Compton time.  $\alpha$  is the fine-structure constant.  $b = 2/(3\chi_e(r, t))\xi/(1-\xi)$  and  $\text{Int}K_{5/3}(b) = \int_b^\infty K_{5/3}(q)dq$ , with  $K_\nu$  the modified Bessel function of the second kind. To employ Eq. (S2) for studying the quantum radiation, the locally constant field approximation (LCFA) is required. The condition for the validity of LCFA in a leptonic collision is analyzed in Sec. III. The LCFA has been verified to be valid for the collisions considered in our study.

Equation (S2) shows that the probability of photon emission is solely determined by the local  $\chi_e(r, t)$  of the emitting particle. It was known that the spectrum of  $d^2W/dtd\xi$  [Eq. (S2)], as a function of  $\xi$ , presents a peak at  $\xi \simeq 1$  for  $\chi_e > 16$  [8, 27, 61]. We further investigated the corresponding power spectrum given by  $\mathcal{E}_0\xi d^2W/dtd\xi$ . The power spectrum is also found to feature a peak at  $\xi = \xi_{peak} \simeq 1$ . We define  $b_{peak} = 2/(3\chi_e)\xi_{peak}/(1-\xi_{peak})$  to characterize the position of this spectral peak.  $b_{peak}$  converges fast to an asymptotic value, i.e.,  $b_{peak} \rightarrow 0.417$ , when  $\chi_e$  increases. This asymptotic value can be obtained by solving  $\partial_b(\xi d^2W/dtd\xi) = 0$  in the limit of  $\chi_e \gg 1$ . If one assumes  $b_{peak} \simeq 0.417$ , the amplitude of this characteristic peak in the power spectrum  $\mathcal{E}_0\xi d^2W/dtd\xi$  emitted from a particle is given by

$$\left( \mathcal{E}_0\xi \frac{d^2W}{dtd\xi} \right)_{peak} \simeq 0.17 \frac{\alpha mc^2}{\tau_c} \chi_e \quad (\text{S3})$$

This scaling is in excellent agreement with the numerical cross-check. Equation (S3) shows an interesting property of this characteristic peak that the peak amplitude is solely determined by  $\chi_e$ .

The time-integrated photon spectrum emitted from a single particle in a beam is given by  $s_\omega(\xi, r) = \int_{-\infty}^\infty (d^2W/dtd\xi)dt$  [26]. The collective spectrum from the whole beam, normalized by the particle number  $N_0$ , is given by

$$\mathcal{S}_\omega(\xi) = \frac{\int_0^\infty s_\omega(\xi, r)f(r)rdr}{\int_0^\infty f(r)rdr} \quad (\text{S4})$$

In order to obtain analytical results for  $\mathcal{S}_\omega(\xi)$ , we will consider two approximations. *The first approximation* is to approximate the special functions in  $d^2W/dtd\xi$  [Eq. (S2)], including  $\text{Int}K_{5/3}(b)$  and  $K_{2/3}(b)$ . *The second approximation* is to approximate the Gaussian beam profile by a uniform profile, which allows to perform the double integral for  $\mathcal{S}_\omega(\xi)$ . These two approximations are detailed and justified in the following.

*The first approximation.* Both  $\text{Int}K_{5/3}(b)$  and  $K_{2/3}(b)$  can be well approximated in the  $\chi_e \gg 1$  regime. In this regime,  $b \ll 1$  for most photon emission. We first approximate the  $K_{2/3}(b)$  term, since it is dominant in determining high- $\xi$  ( $\xi \simeq 1$ ) photon emission which is of our interest in the quantum regime. The asymptotic analysis of  $K_{2/3}(b)$  gives  $K_{2/3}(b) \propto b^{-2/3}$  for  $b \ll 1$ , and  $\propto \exp(-b)$  for  $b \gg 1$ . One can therefore approximate  $K_{2/3}(b)$  as

$$K_{2/3}(b) \simeq k_{2/3}b^{-2/3} \exp(-b) \quad (\text{S5})$$

where  $k_{2/3} \sim \mathcal{O}(1)$  is the fitting coefficient. Because the  $K_{2/3}(b)$  term is critical for high- $\xi$  photon emission, we seek a good approximation of  $K_{2/3}(b)$  which matches the characteristic peak of the power spectrum of radiation  $\mathcal{E}_0\xi d^2W/dtd\xi$  as analyzed before. Because the position of this peak obeys  $b_{peak} \rightarrow 0.417$  in the  $\chi_e \gg 1$  regime, we can set the approximation in Eq. (S5) to match the spectral peak, i.e.,  $K_{2/3}(0.417) = k_{2/3}(0.417)^{-2/3} \exp(-0.417)$ , resulting in  $k_{2/3} = 1.23$ .

The approximation of  $\text{Int}K_{5/3}$  can be obtained as follows. On one hand, for  $b \gg 1$ ,  $\text{Int}K_{5/3}$  has the same scaling with  $K_{2/3}(b)$ , i.e.,  $\text{Int}K_{5/3} \propto \exp(-b)$  [26]. On the other hand, one has the following identity for  $\text{Int}K_{5/3}(b)$ , i.e.,

$$\int_b^\infty K_{5/3}(q)dq \equiv 2K_{2/3}(b) - \int_b^\infty K_{1/3}(q)dq \quad (\text{S6})$$

Because  $K_{2/3}(b) \gg \int_b^\infty K_{1/3}(q)dq$  for  $b \ll 1$ , one can have  $\text{Int}K_{5/3} = \int_b^\infty K_{5/3}(q)dq \simeq 2K_{2/3}(b)$  for  $b \ll 1$ .  $\text{Int}K_{5/3}$  can thus be approximated as

$$\text{Int}K_{5/3} \simeq 2K_{2/3}(b) \simeq 2k_{2/3}b^{-2/3} \exp(-b) \quad (\text{S7})$$

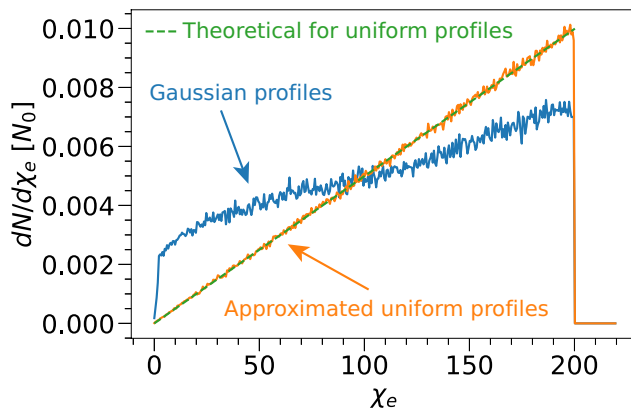


FIG. S1. (Color online).  $dN/d\chi_e$  distribution of the particles in leptonic beam-beam collisions. A Monte Carlo code is developed to simulate these collisions. The colliding beams are represented by pseudo-particles created using random number generation. Each pseudo-particle is assigned with a weight given by the initial local density of the beam. The beams are set to cross each other at the speed of  $c$ . The  $\chi_e(r, t)$  of each particle is calculated based on the local fields from the oncoming beam. The  $dN/d\chi_e$  distribution shown here is taken at the peak interaction moment (when the centers of colliding beams cross) in a collision with  $\chi_{e\max} = 200$ . The distribution is normalized by  $N_0$  (particle number of the beam).  $\sim 10^6$  pseudo-particles are initialized for each colliding beam. Different beam profiles are compared here. The blue line is for Gaussian colliding beams with  $\mathcal{E}_0 = 90$  GeV,  $\sigma_0 = 30.7$  nm,  $\sigma_z = 30.7$  nm, and  $N_0 = 1.37 \times 10^9$ . The orange line is for colliding beams with the approximated uniform profile as specified in Eq. (S8). The green dashed line represents the theoretical distribution for the approximated uniform profile, i.e.,  $dN/d\chi_e = 2\chi_e/\chi_{e\max}^2$ .

*The second approximation.* The Gaussian profile of the colliding beam can be approximated by a uniform cylinder of radius  $\sigma_{0A}$  and length  $\sigma_{zA} = 2\sqrt{2}\sigma_z$ , with a constant density  $n_{0A}$ . The profile of the approximated cylinder is characterized by  $f_A(r) \equiv 1$  for  $r \leq \sigma_{0A}$ , and  $g_A(z) \equiv 1$  for  $z_c - \sigma_{zA}/2 \leq z \leq z_c + \sigma_{zA}/2$ . We further impose the requirement that the approximated uniform profile should match  $\chi_{e\max}$  of the original Gaussian profile. The electric field of the approximated uniform beam is given by  $E_{rA} = 2\pi en_{0A}r$ . The maximum  $E_{rA}$ , given by  $E_{rA, \max} = 2\pi en_{0A}\sigma_{0A}$ , should match the peak field of the original Gaussian beam, leading to  $n_{0A}\sigma_{0A} = 0.9n_0\sigma_0$ . In other words, a collision between round Gaussian beams can be approximated by a collision between beams with the approximated uniform profile specified as:

$$n_{0A}\sigma_{0A} = 0.9n_0\sigma_0, \quad \sigma_{zA} = 2\sqrt{2}\sigma_z \quad (\text{S8})$$

Here, we justify that the approximated uniform profile can preserve the  $\chi_e$  distribution of beam particles in the collision ( $dN/d\chi_e$ ). To study the beamstrahlung from a collision, it is crucial to preserve the  $dN/d\chi_e$  distribution of beam particles, as the radiation probability [Eq. (S2)] is solely determined by  $\chi_e(r, t)$  of the emitting particle. Figure S1 depicts the  $dN/d\chi_e$  distribution at the peak interaction moment (when the centers of colliding beams cross) in a collision with  $\chi_{e\max} = 200$ . A Monte Carlo code is developed to simulate beam-beam collisions where the  $dN/d\chi_e$  distribution can be calculated, as explained in the figure caption. The theoretical  $dN/d\chi_e$  distribution of colliding beams with the approximated uniform profiles can be analytically given, i.e.,  $dN/d\chi_e = 2\chi_e/\chi_{e\max}^2$  (green line), and it is perfectly verified by the Monte Carlo result (orange line). The approximated uniform profile can largely preserve the shape and amplitude of  $dN/d\chi_e$  distribution, compared with those of original Gaussian profiles. This preservation assures that the quantum radiation calculated with the approximated uniform profile can well reflect the radiation from Gaussian colliding beams.

*The collective radiation spectrum  $\mathcal{S}_\omega(\xi)$ .* As analyzed in *the second approximation*, the radiation from a collision between round Gaussian beams can be approximated by that from a collision between the uniform cylindrical beams as specified in Eq. (S8). With the approximated uniform profile, the corresponding  $\chi_e$  is given by  $\chi_{eA} = 2\gamma E_{rA}/E_s$ , and the  $b$  parameter in  $d^2W/dtd\xi$  [Eq. (S2)] is given by

$$b = \frac{2}{3\chi_{eA}(r, t)} \frac{\xi}{1 - \xi} = \frac{2}{3\chi_{e\max}} \frac{\xi}{1 - \xi} \frac{\sigma_{0A}}{r} = b_0 \frac{\sigma_{0A}}{r} \quad (\text{S9})$$

where  $b_0 = 2/(3\chi_{e\max})\xi/(1 - \xi)$ .



The normalized collective spectrum  $\mathcal{S}_\omega(\xi)$  is therefore calculated as

$$\begin{aligned}
\mathcal{S}_\omega^{Gaussian}(\xi) &= \int_0^\infty s_\omega(\xi, r) f(r) r dr / \int_0^\infty f(r) r dr \\
&\simeq \mathcal{S}_\omega^{Approximated}(\xi) \\
&= \int_0^{\sigma_{0A}} s_{\omega A}(\xi, r) f_A(r) r dr / \int_0^{\sigma_{0A}} f_A(r) r dr \\
&= \int_0^{\sigma_{0A}} \left( \int_0^{\sigma_{zA}/2c} \frac{d^2 W}{dt d\xi} dt \right) f_A(r) r dr / \int_0^{\sigma_{0A}} f_A(r) r dr \\
&= \frac{2\sqrt{2}\alpha\sigma_z}{\sqrt{3}\pi\tau_c\gamma c} k_{2/3} \left( 2 + \frac{\xi^2}{1-\xi} \right) b_0^2 \Gamma \left[ -\frac{8}{3}, b_0 \right]
\end{aligned} \tag{S10}$$

where  $\Gamma$  is the incomplete Gamma function [56, 57]. Equation (S10) is shown to give the accurate photon emission in both the  $\chi_{e\max} \sim 1$  and the  $\chi_{e\max} > 1$  regimes. This is confirmed by the numerical calculation of  $\mathcal{S}_\omega(\xi)$  without employing approximations, i.e., using the exact  $d^2W/dtd\xi$  in Eq. (S2) and original Gaussian beam profiles. In addition, Equation (S10) is also verified by 3-dimensional (3D) QED particle-in-cell (PIC) simulations as shown in the main text.

## II. THREE-DIMENSIONAL (3D) QED PARTICLE-IN-CELL (PIC) SIMULATIONS FOR LEPTONIC COLLISIONS

In this Section, we give details of 3-dimensional (3D) particle-in-cell (PIC) simulations with code OSIRIS [58] employed to study leptonic beam-beam collisions. The relevant strong-field QED (SF-QED) effects, including nonlinear Compton scattering (quantum synchrotron radiation) and electron-positron pair creations from multiphoton Breit-Wheeler process, are self-consistently added to the particle dynamics in this QED-PIC code [59, 60, 62, 78]. The PIC simulation shown in the main text studies a head-on collision between two identical, cold, round, and Gaussian electron beams with  $\chi_{e\max} = 200$ . Each beam has energy  $\mathcal{E}_0 = 90$  GeV, longitudinal length  $\sigma_z = 30.7$  nm, transverse size  $\sigma_0 = 30.7$  nm, and particle number  $N_0 = 1.37 \times 10^9$ . In the simulation, two beams are counterpropagating in  $z$  direction, with their densities initialized as  $n_1 = n_0 \exp(-(x^2 + y^2)/2\sigma_0^2) \exp(-(z + 3\sigma_z)^2/2\sigma_z^2)$  for  $-6\sigma_z \leq z \leq 0$ , and  $n_2 = n_0 \exp(-(x^2 + y^2)/2\sigma_0^2) \exp(-(z - 3\sigma_z)^2/2\sigma_z^2)$  for  $0 \leq z \leq 6\sigma_z$ , respectively, where  $n_0 = 3 \times 10^{24} \text{ cm}^{-3}$  is the peak density. The transverse distribution of the beam is truncated at  $3\sigma_0$ , i.e.,  $\sqrt{x^2 + y^2} \leq 3\sigma_0$ . The size of computation cells is given by  $dz = 0.6 \text{ nm} = 0.02\sigma_z$  and  $dx = dy = 0.46 \text{ nm} = 0.015\sigma_0$ . The time step is  $dt = 0.009\sigma_z/c$ . The number of macro particles of each beam is  $7.7 \times 10^7$ . The simulation lasts until  $t = 6\sigma_z/c$  when the beams completely cross each other. The locally constant field approximation (LCFA) has been verified to be valid for the collision studied here, as shown in Sec. III.

## III. THE VALIDITY OF THE LOCALLY CONSTANT FIELD APPROXIMATION (LCFA) IN LEPTONIC COLLISIONS

In this Section, we analyze the validity of LCFA in leptonic collisions. The LCFA is valid when the relevant formation length is much shorter than the scale length at which the collective background fields vary [12]. In the quantum regime, the formation length  $l_f$  for photon emission in a collision is  $l_f \sim \lambda_c \gamma \chi_{e\max}^{-2/3}$  where  $\lambda_c = \hbar/mc = 3.86 \times 10^{-11} \text{ cm}$  is the reduced Compton length. For a beam-beam collision, the scale length of background fields is the beam length  $\sigma_z$ . Therefore, the LCFA is valid when  $l_f \ll \sigma_z$ . For the collision studied in Sec. II,  $\chi_{e\max} = 200$ , and  $l_f \sim 2 \text{ nm} \ll \sigma_z = 30.7 \text{ nm}$ , leading to a valid LCFA.

After some algebra, the condition  $l_f \ll \sigma_z$  for a valid LCFA can be expressed as

$$\left( \frac{\sigma_0}{d_e} \right)^{2/3} \frac{\sigma_z}{d_e} \gg \left( \gamma \frac{\lambda_c}{d_e} \right)^{1/3} \tag{S11}$$

where  $d_e = c/\omega_p$  is the electron skin depth, with  $\omega_p = \sqrt{4\pi n_0 e^2/m}$  the plasma frequency at the peak density of the beam. For dense beams employed in our study, the beam dimensions ( $\sigma_0$  and  $\sigma_z$ ) are much larger than  $d_e$ , and the condition Eq. (S11) can thus be well satisfied.

#### IV. THEORETICAL ESTIMATION OF THE SPECTRAL BRIGHTNESS OF THE GAMMA-RAY BEAMS EMITTED FROM LEPTONIC COLLISIONS

In this Section, we derive the theoretical estimation of the spectral brightness of gamma-ray beams emitted from leptonic collisions. The spectral brightness of a photon beam is defined as [68]

$$B(\xi) = \frac{\frac{dN_\gamma}{dt}}{4\pi^2\sigma_x\sigma_y\sigma_{x'}\sigma_{y'}\frac{\Delta\omega}{\omega}} \quad (\text{S12})$$

where  $dN_\gamma/dt$  is the photon flux (per second) at a specific photon frequency  $\omega$  with a bandwidth  $\Delta\omega/\omega$ . Here,  $\Delta\omega/\omega = \Delta\xi/\xi$ , as  $\xi = \mathcal{E}_\gamma/\mathcal{E}_0 = \hbar\omega/\mathcal{E}_0$ . In the community of synchrotron light source, the bandwidth is usually chosen to be  $\Delta\xi/\xi = 0.1\%$ .  $\sigma_x$  and  $\sigma_y$  are root mean square (RMS) values of transverse sizes of the photon beam in the  $x$  and  $y$  directions, respectively.  $\sigma_{x'}$  and  $\sigma_{y'}$  are the corresponding RMS values of solid angles (momentum divergence of the photon beam).

The number of photons at energy  $\xi$  with a specific bandwidth  $\Delta\xi/\xi$  is given by

$$N_\gamma(\xi) = N_0\mathcal{S}_\omega(\xi)\Delta\xi = N_0\xi\mathcal{S}_\omega(\xi)\frac{\Delta\xi}{\xi} \quad (\text{S13})$$

This relation shows that  $N_\gamma(\xi) \propto \xi\mathcal{S}_\omega(\xi)$  when  $\Delta\xi/\xi$  is fixed. Therefore, one has  $B(\xi) \propto \xi\mathcal{S}_\omega(\xi)$ , assuming that photons at different energy  $\xi$  have the same pulse duration. Since  $B(\xi) \propto \xi\mathcal{S}_\omega(\xi)$ , the spectral brightness will also feature a sharp peak ( $B_{peak}$ ) at  $\xi = \xi_{peak} \simeq 1$ , as shown in the  $\xi\mathcal{S}_\omega$  spectrum. Using Eq. (S13), the number of photons at energies  $[\xi_{peak}, \xi_{peak} + \Delta\xi]$  is simply given by

$$N_\gamma(\xi_{peak}) = N_0P_{\xi\mathcal{S}_\omega}\frac{\Delta\xi}{\xi_{peak}} \quad (\text{S14})$$

where  $P_{\xi\mathcal{S}_\omega}$  is the amplitude of the peak in the  $\xi\mathcal{S}_\omega$  spectrum.  $P_{\xi\mathcal{S}_\omega}$  is given in the main text.

The emitted photon beam has the same emittance, including the spatial size and solid angles, with the emitting beam in a collision. This allows us to conveniently set  $\sigma_x = \sigma_y \simeq \sigma_0$  and  $\tau_\gamma \simeq 2\sqrt{2}\sigma_z/c$ , where  $\tau_\gamma$  is the pulse duration of the photon beam. The divergence angle of the photon beam can be approximated as the deflection angle of the beam particles, due to the disruption effect caused by the fields from the oncoming beam [54]. The deflection angle of a particle with the initial position  $r = r_0$  is calculated as  $\theta_0(r_0) = r_e N_0 r_0 / (\gamma \sigma_0^2)$  [54] where  $r_e = e^2/mc^2$  is the classical electron radius. Because the particles at  $r \simeq r_{peak}$  are subject to the peak fields of the oncoming beam, these particles undergo fastest and strongest quantum radiation. Here,  $r_{peak}$  depicts the position of the peak fields. For a Gaussian beam,  $r_{peak} = 1.6\sigma_0$ . We employ the deflection angle of particles at  $r \simeq r_{peak}$  to estimate the divergence angle of the radiated photon beam, i.e.,

$$\sigma_{x'} = \sigma_{y'} \simeq \theta_0(r \simeq r_{peak}) \simeq \frac{r_e N_0 r_{peak}}{\gamma \sigma_0^2} \quad (\text{S15})$$

This divergence estimation agrees well with the 3-dimensional (3D) particle-in-cell (PIC) simulations.

With the above analysis, the peak spectral brightness at  $\xi = \xi_{peak}$  is estimated as

$$\begin{aligned} & \frac{B_{peak}(\xi_{peak})}{\text{photons}/(\text{s mm}^2 \text{ mrad}^2 \text{ 0.1\%BW})} \\ &= \frac{N_\gamma(\xi_{peak})/\tau_\gamma}{4\pi^2\sigma_x\sigma_y\sigma_{x'}\sigma_{y'}\Delta\xi/\xi_{peak}} \\ &\simeq 3.87 \times 10^{32} \frac{\gamma}{N_0} \chi_{e\max} \\ &= 1.16 \times 10^{26} \frac{(\mathcal{E}_0[\text{GeV}])^2}{\sigma_0[0.1\mu\text{m}] \sigma_z[0.1\mu\text{m}]} \end{aligned} \quad (\text{S16})$$

Equation (S16) provides a good estimation for the peak brightness of beamstrahlung photons in both the  $\chi_{e\max} \sim 1$  and the  $\chi_{e\max} > 1$  regimes. This is confirmed by 3D PIC simulations.